Al-Khwarizmi Engineering Journal,Vol. 12, No. 1, P.P. 15- 25 (2016)

Al-Khwarizmi Engineering Journal

Experimental Study of the Performance of Compound Parabolic Concentrating Solar Collector

Qussai Jihad Abdul-Ghafour* **Mohammed Aziz Hassan****

*,** *Department of Mechanical Engineering / University of Technology*

* Email: kaisyqj@yahoo.com

** Email: mohammedeng37@gmail.com

(Received 26 April 2015; accepted 4 August 2015)

Abstract

The design, construction and investigation of experimental study of two compound parabolic concentrators (CPCs) with tubular absorber have been presented. The performance of CPCs have been evaluated by using outdoor experimental measurements including the instantaneous thermal efficiency. The two CPCs are tested instantly by holding them on a common structure. Many tests are conducted in the present work by truncating one of them in three different levels. For each truncation the acceptance half angle (θ_c) was changed. Geometrically, the acceptance half angle for standard CPC is (26^o). For the truncation levels for the other CPC 1, 2 and 3 the acceptance half angle were 20^o, 26^o and 59^o, consequently. A significant difference between the instantaneous thermal efficiency of 3.86× CPC (θ_c=20^o) and 2.32× CPC (θ_c=26^o), and between that for 3.61× CPC (θ_c=26^o) and 2.32× CPC (θ_c=26^o). It's noticed that the difference between the instantaneous thermal efficiency of 2.32× CPC (θ_c=59^o) and 2.32× CPC (θ_c=26^o) is small compared with the difference of the first and second cases, the instantaneous thermal efficiency of 2.32× CPC (26^o) was higher than those for other three CPCs. The experimental results show that the maximum thermal efficiency of the full 2.32×CPC (26^o) is 0.708, the maximum thermal efficiency of the 3.93×CPC (15^o), when it's truncated to 3.84× CPC (20^o), 3.61× CPC (26^o) and 2.32× CPC (59^o) are 0.51, 0.52 and 0.66, respectively. As the concentration ratio decreases from (3.93× to 1×), the thermal efficiency, energy losses and optical efficiency increase from (0.47 to 63), (1.58 to 7.2 K.m^2/W) and (0.494 to 0.797), respectively.

Keywords: *CPC collector, truncation effect, thermal performance.*

1. Introduction

Compound Parabolic Concentrator consists of two different parabolic reflectors that can reflect both direct and a fraction of the diffuse radiation incident at the entrance aperture onto the absorber in addition to the direct solar radiation absorbed directly by the absorber [1]. CPC collectors can accept incoming solar radiation over a relatively wide range of incidence angles. By using multiple internal reflections of ray, any radiation entering the collector's aperture within the CPC acceptance angle finds its way to the absorber surface located at the bottom of the collector [2].

Since the invention of the compound parabolic concentrator (CPC), many researchers have been published that deal with a wide range of designs and analysis of this system. However, a close examination of these researches reveals that the great majority of them are devoted to the geometrical, optical and thermal analysis of the CPC with a tubular receiver.

McIntire, 1979 [3], studied the truncation of non-imaging cusp reflectors which concentrate sunlight onto cylindrical absorbers. presented the shapes of reflector for truncated CPC concentrators having various acceptance angles. Finally, concluded that the truncation leads to collector designs which are more cost effective through substantial reductions in mirror height and length with small reductions in concentration ratios. Gordon, et al., 1985 [4], derived analytic expressions for the angular acceptance function of two-dimensional CPCs of arbitrary truncation degree. took into account the effect of truncation on both optical and thermal losses in real

collectors, also evaluated the monthly and yearly collectible energy increasing. Concluded that yearly collectible energy increased and average number of reflection reduced with truncation. Suzuki and Kobayashi 1995 [5], studied the optimum acceptance angle of a CPC by the use of an insolation model. The yearly insolation model suggested that the optimum half-acceptance angle at the two-dimensional CPC becomes 26° irrespective of the change of the diffuse radiation fraction. Concluded that, a common CPC could be used as an optimum concentration, almost all over the world. Winston and O'Gallagher 2004 [6], studied the performance of the non-imaging solar collectors CPC with tubular absorber (evacuated and selective surface), empirically in two groups with different concentrating ratio, the first low (1.1×-1.4×) and the other high (about 5×). They found that the first group don't needed diurnal tracking and its efficiency 40% at 150^{o}C. The second needed monthly tilt adjustment and its efficiency 60% at 220^{o}C. Tang, et al., 2010 [7], developed a mathematical procedure to estimate the annual collectible radiation captured by fixed CPC oriented in east-west direction based on the monthly horizontal radiation. Results showed that the optimal acceptance half-angle for maximizing CPC's annual energy collection was 25.97^{o}, and the yearly optimal tilt-angle of apertures relative to the horizon was equal to the site latitude.

The aim of the present work is to evaluate the performance of the full CPC collector with different truncation levels and comparing the results with standard CPC collector with (26^{o}) acceptance half angle.

2. Description of the CPC

Two models of CPCs have been adopted, manufactured and tested at a totally sunny space. These models consisted of a support structure that allows to position the CPCs at different angles, reflector parts assembly and evacuated tube absorbers as shown in Fig. 1. The evacuated tube is used in this work as the absorber part. It consist of a double glass concentric tubes and the space between them is evacuated in order to reduce the convection losses. The inner tube is treated by a selective coating with specifications tabulated in Table 1. Fig. 2. Show a schematic diagram of the evacuated tube [8]. Geometrical characteristics of the designed CPC collector, are given in Table 2. The previous researchers used number of CPCs models, symmetric and axisymmetric, with and without transparent cover on the aperture, North-South and East-West axis oriented as shown in Fig. 3. In this present work the CPCs used are symmetric, without transparent cover plate and oriented E-W, south facing.

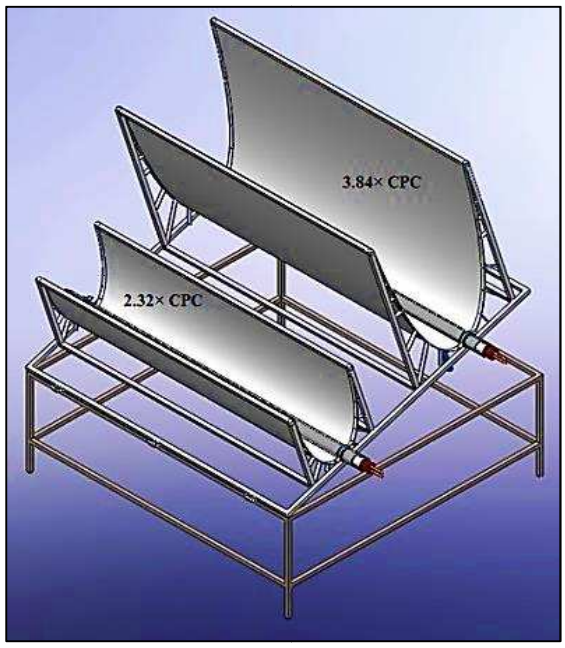

Fig. 1. The schematic of CPC collectors.

Table 1,
Evacuated tube specifications [8].

Parameters	Units	Values
Receiver length	mm	1800
Cover diameter	mm	58
Absorber diameter	mm	47
Cover Transmittance	%	91
Coated surface absorptance	%	93
Coated surface emittance	%	<8
Pressure of vacuum space	Pa	5×10^{-3}
Heat Loss	W/m^2°C	< 0.8
Insolation Temp.	°C	250

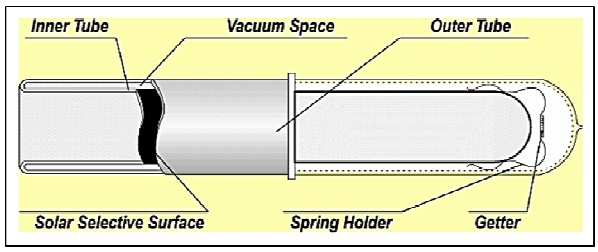

Fig. 2. Schematic diagram of the Evacuated tube.

Table 2,
The geometrical characteristics of the designed CPC collectors.

Parameters	Units	2.32× CPC	3.84× CPC		
Acceptance half-angle	Deg.	26	15		
Truncation	Deg.	Full CPC	20	26	59
Geometric concentration ratio	--	2.32	3.84	3.61	2.32
Aperture area	m^2	0.512	0.848	0.797	0.512
Aperture width	m	0.343	0.567	0.533	0.343
Length of the CPC	m	1.495	1.495		

CPC's support structure consists of two group assemblies: stationary base assembly, in order to undergo the hard weather conditions, and achieve

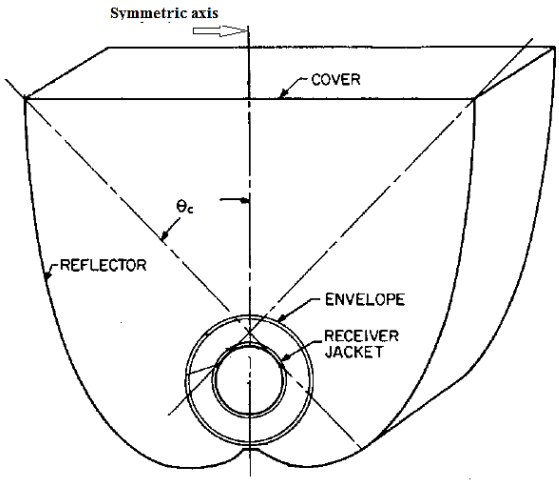

Fig. 3. Schematic diagram of the CPC with transparent cover and symmetric axis.

The supporting requirement through the solar energy collectors operation. And the other, tilting part assembly where the CPCs supported on, it allows to position the CPCs at different tilt angles. The reflector is designed to set the acceptance half angle 15° and truncated in three levels, to 20° (3.84× CPC), 26° (3.61× CPC) and 59° (2.32× CPC) as illustrated in Fig. 4. A second reflector is designed to set acceptance half angle 26° (2.32× CPC) as illustrated in Fig. 5. Cartesian coordinate system and the optical axis of the concentrator as the y-axis, the two sections: involution and reflection sections of the reflector curves are drawn separately to achieve the ideal concentration ratio as shown in Fig. 6. Any point on the reflector is [9]:

$$x = r\sin\theta - \rho(\theta)\cos\theta \quad \ldots(1)$$

$$y = -r\cos\theta - \rho(\theta)\sin\theta \quad \ldots(2)$$

where : $\rho(\theta)$ for $\theta_m \le |\theta| \le \theta_c + \pi/2$:

$$\rho(\theta) = (r + l_g)\sin\theta_m + r(\theta + \theta_m) \quad \ldots(3)$$

For $\theta_c + \pi/2 \le \theta \le 3\pi/4 - \theta_c$:

$$\rho(\theta) = \frac{r(\theta_c + \frac{\pi}{2} + \theta - 2\theta_m + 2\tan\theta_m - \cos(\theta - \theta_c))}{1 + \sin(\theta - \theta_c)} \quad \ldots(4)$$

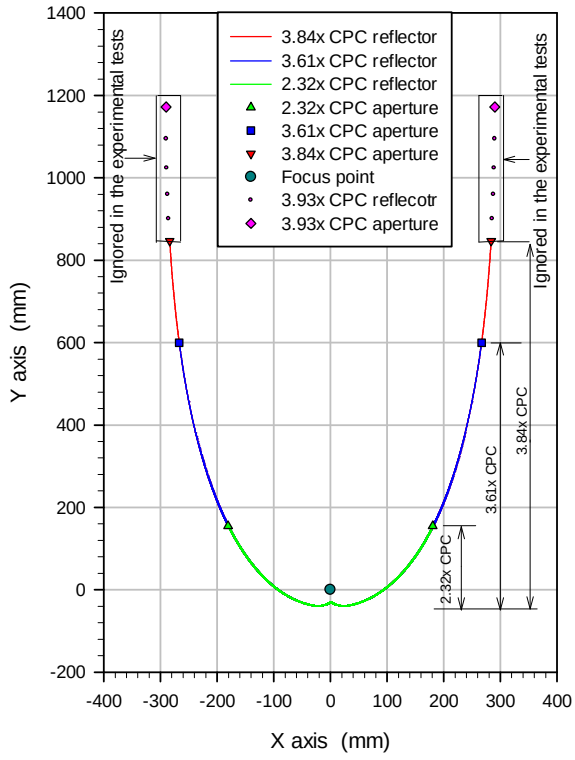

Fig. 4. Illustration of designed 3.84× CPC.

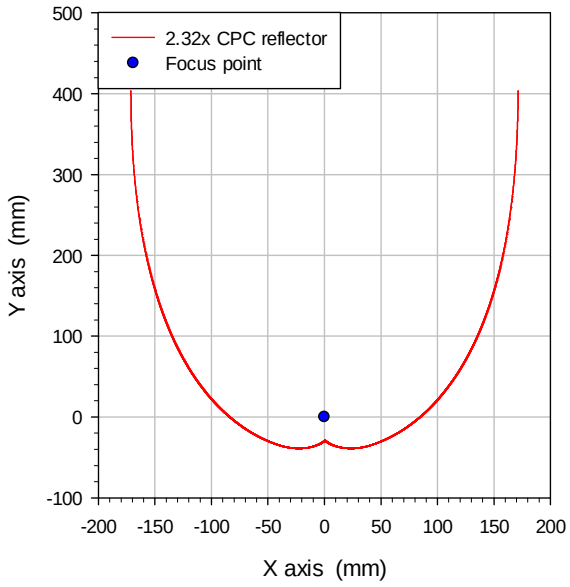

Fig. 5. illustration of designed 2.32× CPC.

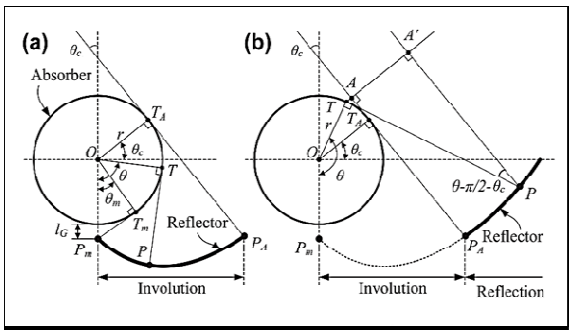

Fig. 6. Two sections of CPC: (a) Involution (b) Reflection [9].

3. Experimental Setup and Performance Indexes

3.1. Experimental Setup

The experimental unit has the following elements as shown in Fig. 7. : (1)2.32× CPC, (2) 3.84× CPC,(3) Two 48 liter storage tanks, one for each CPC, and (4) Two circulating pumps, with mass flow rate of 0.02 kg/s, the circulation pump had two functions, which were (i) homogenization the water temperature in the storage tank by breaking up the stratification of the water, and (ii) circulating the water through the CPC absorber tube at constant mass flow rate. A flexible tubes are used for conveyance of the water. To investigate the thermal performance of CPCs, the water temperatures at inlet and outlet of the absorber tubes, the temperature of the storage tank, and solar radiation intensity (beam and diffuse) are measured during the experiments.

3.2. Performance Indexes

The optical performance of CPC collectors can be analyzed theoretically, by obtaining values of the optical efficiency and incidence angle modifier (IAM) with respect to incidence angle projections, by using ray tracing software. And to evaluate thermal performance of the 2.32×CPC and 3.84× CPC collectors, thermal efficiency must be considered. The data for the beam and diffuse solar radiations and useful heat gain by the CPCs were obtained previously to determine the instantaneous and daily efficiencies η_{th}.

3.2.1. Optical Efficiency

Optical efficiency obtained by using three dimensional ray tracing program TRACE PRO [10]. To simulate solar radiation above the plane of the collector, 1000 rays are randomly distributed over the width of the aperture. The fraction of impacted rays on the absorber gives an optical efficiency value for an incidence angle.

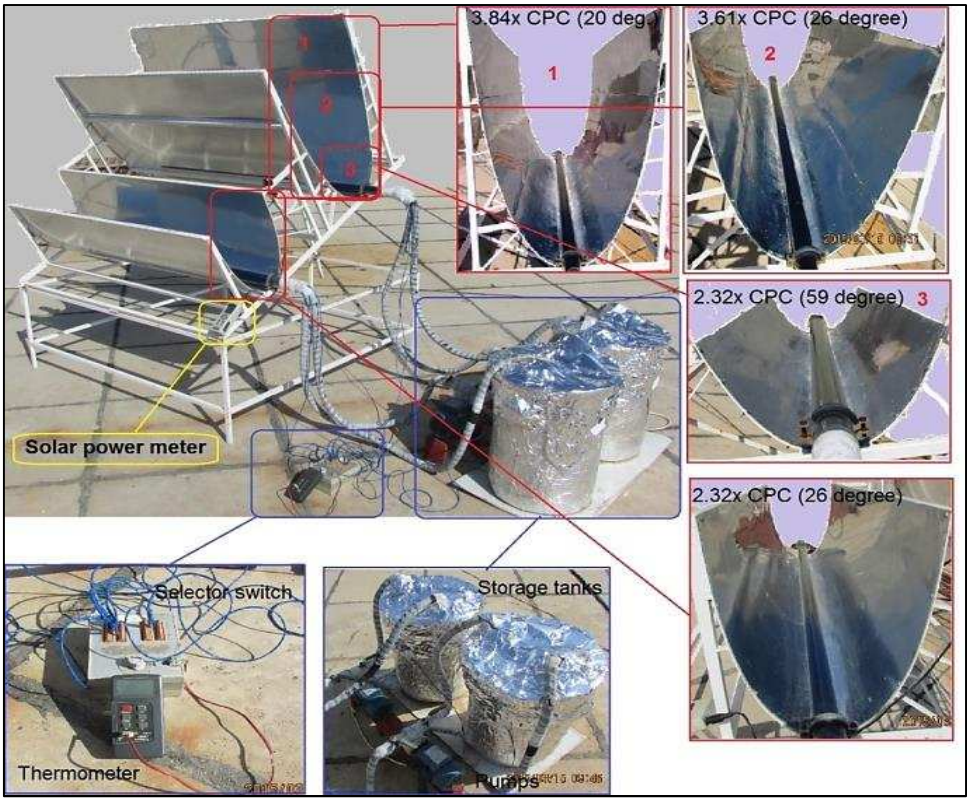

Fig. 7. A photograph of CPCs setup.

3.2.2. Thermal Efficiency

The CPC instantaneous thermal efficiency of the CPCs for three cases (i) 3.86× CPC (θ_c=20^o) and 2.32× CPC (θ_c=26^o), (ii) 3.61× CPC (θ_c=26^o) and 2.32× CPC (θ_c=26^o), and (iii) 2.32× CPC (θ_c=59^o) and 2.32× CPC (θ_c=26^o), are computed from Eq. (5).

$$\eta_{th} = \frac{Q_u}{A_a I_t} \quad \ldots (5)$$

where Q_u, is the heat gain by the collector, and calculated from Eq.(6). [11]:

$$Q_u = \dot{m} C_p (T_o - T_i) \quad \ldots (6)$$

The thermal efficiency of CPC can be described by ASHRAE Standard 93-2010 [12], as demonstrated in Eq.(5). If the thermal efficiency (The Performance Curve of CPC) from Eq. (5) is plotted against the temperature difference between fluid inlet temperature and ambient temperature in relation with the solar irradiance received. The slope of this line represents the heat losses, and its intersection with the vertical axis is an indicator of the optical efficiency without thermal losses.

4. Results and Discussion

The effects of various parameters on the optical and thermal performance of the CPCs are analyzed. The thermal efficiency results were obtained from ray tracing program for optical efficiency, and from outdoor experimental tests through the selected clear-sky days of June, December /2014 and January/2015, for test period extended from 9:00 to 14:00. The mass flow rate used in standard test is in the range between (0.0138-0.0277 kg/s) [12]. The mass flow rate used in the present work is (0.02 kg/s), measured by collecting water in a calibrated cylinder per time measured by a stop watch.

4.1. Analysis of Optical Efficiency

Optical efficiencies and the angular acceptance at any given incident angle are shown in Figures 8 and 9, respectively. Fig. 8 presents the variations of optical efficiencies and the angular acceptance as the transversal projection angle θ_t varies, while θ_l is kept a constant of zero. For truncation, some rays incident at angles beyond the acceptance half-angle hit the receiver directly and others hit the receiver after reflection from the near side of the CPC while rays incident on the far side of the

CPC are rejected over the receiver. The optical efficiencies have a similar trend with the angular acceptance. However, the values of optical efficiencies are always lower than that of the angular acceptance at any transversal angle. Average number of reflections has maximum value at normal incidence angle and decreases in the range (0^o and $\pm\theta_c$).

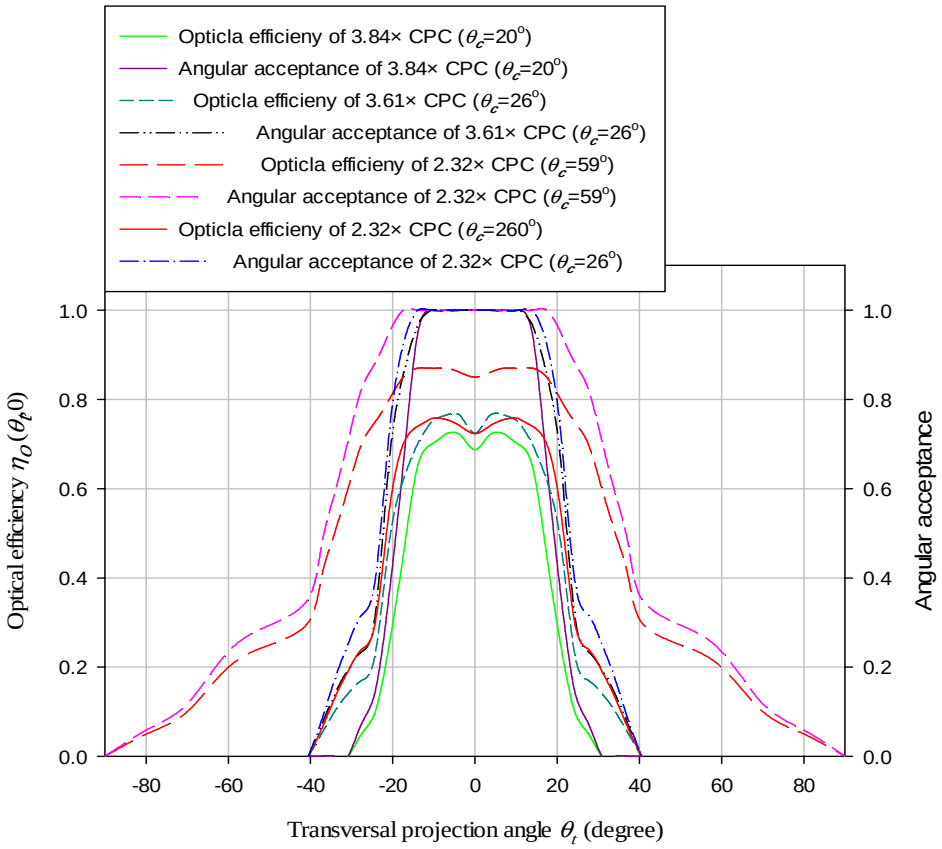

Fig. 8. The optical efficiencies and angular acceptance at different transversal projection angle.

Correspondingly, Fig. 9 shows the effects on the optical efficiency as θ_l varies, while θ_t is fixed at zero. The major optical effects which might be presented in the longitudinal direction are those related with the angular variation of transmittance, absorptivity properties and with radiation spilling or end-mirror reflection effects. Optical efficiency of 3.84× CPC (20^o), 3.61× CPC (26^o), 2.32× CPC (59^o) and 2.32× CPC (26^o) reduces slowly within the range of (-30^o and $+30^o$), (-35^o and $+35^o$), (-50^o and $+50^o$), and (-40^o and $+40^o$), respectively. However, it decreases rapidly beyond this range except the optical efficiency of 3.84× CPC (20^o), it decreases in the range (±30 and ±60) more than the decreasing in the range (-30^o and $+30^o$). The optical efficiencies of 0.684, 0.685, 0.723 and 0.723 at the normal incident angles can be received within the acceptance limit for the 3.84× CPC (20^o), 3.61× CPC (26^o), 2.32× CPC (59^o) and 2.32× CPC (26^o), respectively. The optical efficiency of CPCs has maximum value at normal incident angle due to minimum average number of reflections, and the last increases from (0^o to $\pm90^o$) leads to decreasing the optical efficiency.

Incident angles of CPC collectors results are shown in Fig. 10.

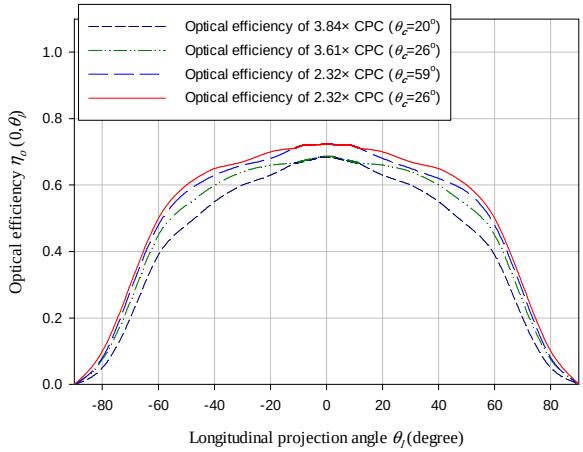

Fig. 9. The optical efficiencies at different longitudinal projection angle.

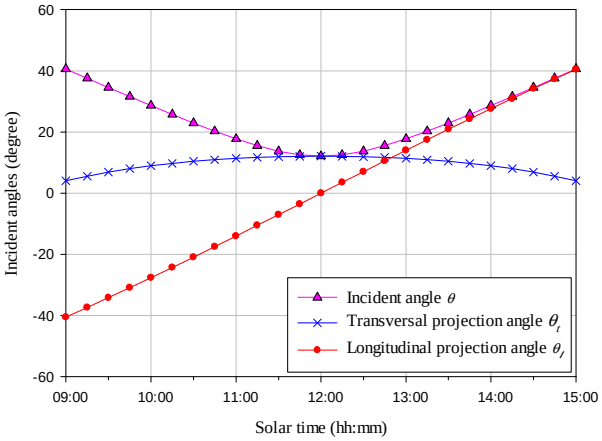

Fig. 10. Incident angles of CPC collectors versus solar time.

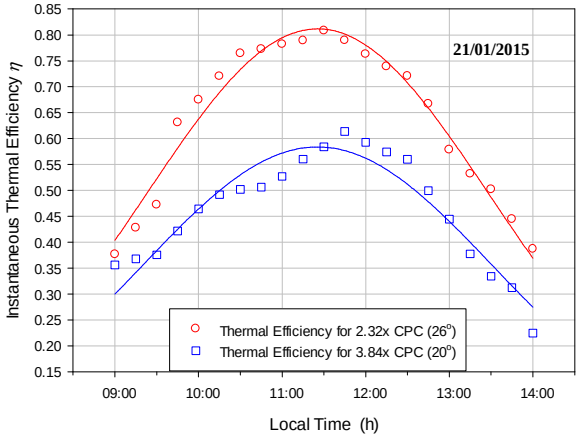

Fig. 11. Variation of instant. efficiency with time for 3.86× CPC (20°) and 2.32× CPC (26°).

4.2. Analysis of Thermal Efficiency

4.2.1. Instantaneous Thermal Efficiency

The efficiency of the CPCs for three cases described previously in section (2.2.1) are plotted in Fig. 11, Fig. 12 and Fig. 13, during the test hours from 09:00 to 14:00 for different days under the same test conditions (inlet temperature, mass flow rate, total solar radiation and ambient temperature). For the first case, Fig. 11 shows that the efficiency of 3.86× CPC (θ_c=20°) is almost lower than that of 2.32× CPC (θ_c=26°) during whole test hours. Since, the optical efficiency of the 2.32× CPC is much higher than that of the 3.86× CPC. For second case, Fig. 12 shows that the efficiency of 3.61× CPC (θ_c=26°) is lower than that of 2.32× CPC (θ_c=26°) with difference lower than that in the first case. Here, the optical efficiency of 2.32× CPC is higher than that of 3.61× CPC and the last has optical efficiency little high than that of 3.86× CPC. For the third case, Fig. 13 shows that the efficiency of 2.32× CPC (θ_c=59°) is close to that of 2.32× CPC (θ_c=26°). So, the optical efficiency of 2.32× CPC (θ_c=26°) has a good agreement with that of 2.32× CPC (θ_c=59°).

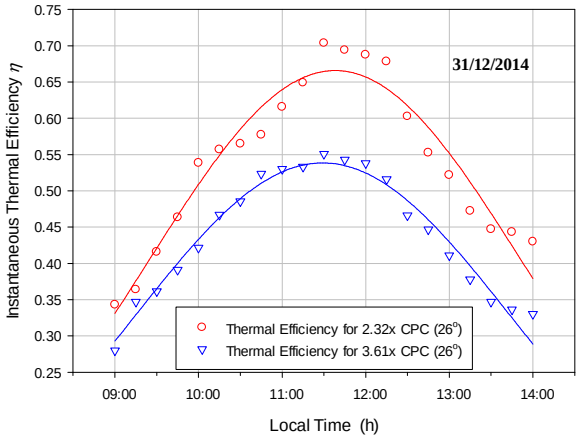

Fig. 12. Variation of instant. efficiency with time for 3.61× CPC (26°) and 2.32× CPC (26°).

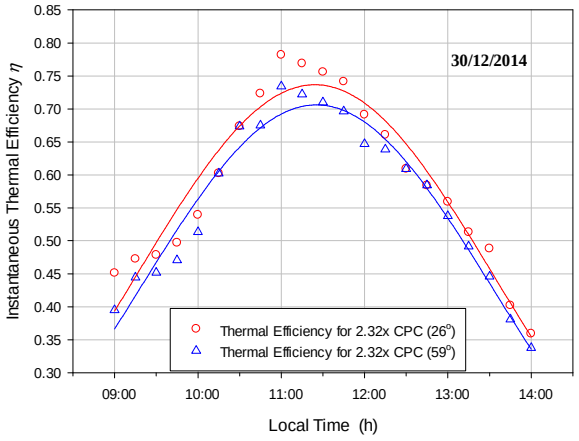

Fig. 13. Variation of instant. efficiency with time for 2.32× CPC (59°) and 2.32× CPC (26°).

4.2.2. The Collector Performance Curves of CPCs

Before tests, the system is cleaned up and the pump is switched on for one hour until reaching steady state. After that, the temperatures of the inlet and outlet water and solar intensity are recorded. Tests were conducted to generate the thermal efficiency curves of CPCs, two tests for every case. The Performance Curves of 3.86× CPC (20°) and 2.32× CPC (26°) are shown in Fig. 14. The empirical equation of thermal efficiency of 3.86× CPC (20°) can be written as:

$$\eta_{th} = -1.8667(T_i - T_a/I_t) + 0.5077 \quad \ldots(7)$$

with R^2=0.996

The empirical equation of thermal efficiency of 2.32× CPC (26°) can be written as:

$$\eta_{th} = -3.4425(T_i - T_a/I_t) + 0.7203 \quad \ldots(8)$$

with R^2=0.996

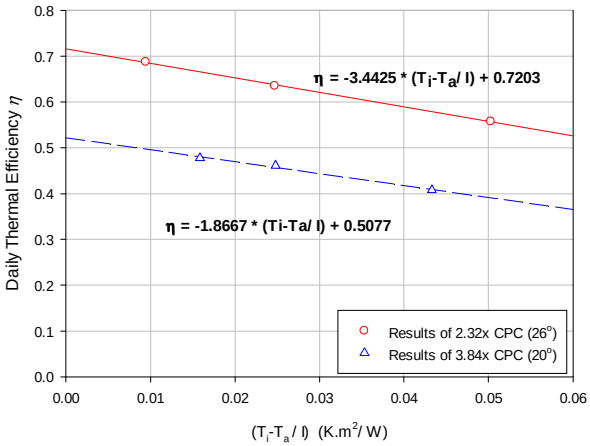

Fig. 14. Thermal efficiency curves of 3.86× CPC (20°) and 2.32× CPC (26°).

The Performance Curves of 3.61× CPC (26°) and 2.32× CPC (26°) are shown in Fig. 15. The empirical equation of thermal efficiency of 3.61× CPC (26°) can be written as:

$$\eta_{th} = -2.0283(T_i - T_a/I_t) + 0.5196 \quad \ldots\ldots..(9)$$

with R^2=0.966

The empirical equation of thermal efficiency of 2.32× CPC (26°) can be written as:

$$\eta_{th} = -3.4449(T_i - T_a/I_t) + 0.6672 \quad \ldots\ldots..(10)$$

with R^2=0.998

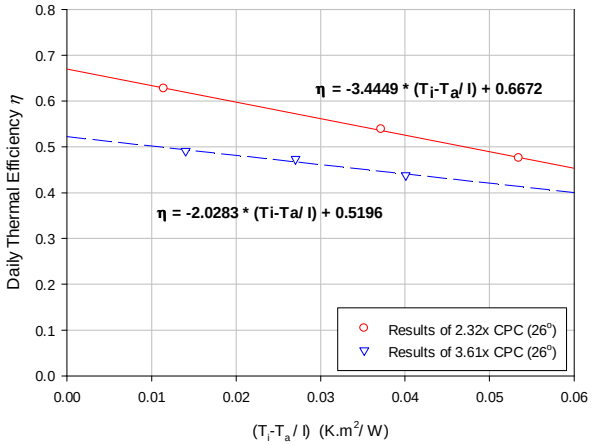

Fig. 15. Thermal efficiency curves of 3.61× CPC (26°) and 2.32× CPC (26°).

The Performance Curves of 2.32× CPC (59°) and 2.32× CPC (26°) are shown in Fig. 16. The empirical equation of thermal efficiency of 2.32× CPC (59°) can be written as:

$$\eta_{th} = -4.7044(T_i - T_a/I_t) + 0.6621 \quad \ldots(11)$$

with R^2=0.999

The empirical equation of thermal efficiency of 2.32× CPC (26°) can be written as:

$$\eta_{th} = -3.9057(T_i - T_a/I_t) + 0.672 \quad \ldots(12)$$

with R^2=0.998

Since, the higher thermal efficiency of the 2.32× CPC (26°) can be realized as a result of the better value of optical efficiency.

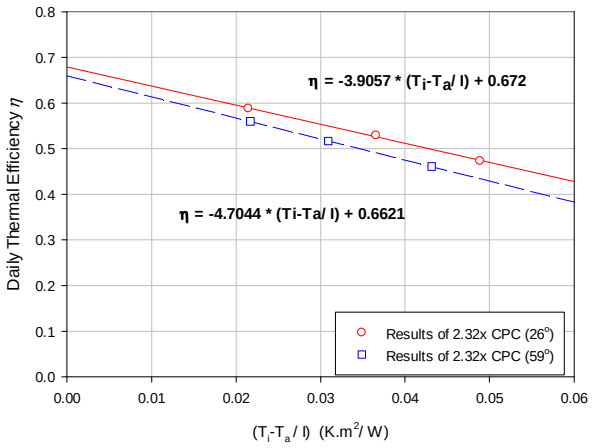

Fig. 16. Thermal efficiency curves of 2.32× CPC (59°) and 2.32× CPC (26°).

4.2.3. The performance curve of 2.32× CPC (26°)

The tests have been conducted over six clear sky days to generate the thermal efficiency curve of 2.32× CPC (26°), which is shown in Fig. 17.
The empirical equation of thermal efficiency of 2.32× CPC (26°) during six tests, can be written as:

$$\eta_{th} = -4.6164(T_i - T_a/I_t) + 0.7095 \quad \ldots(13)$$

with R^2=0.81

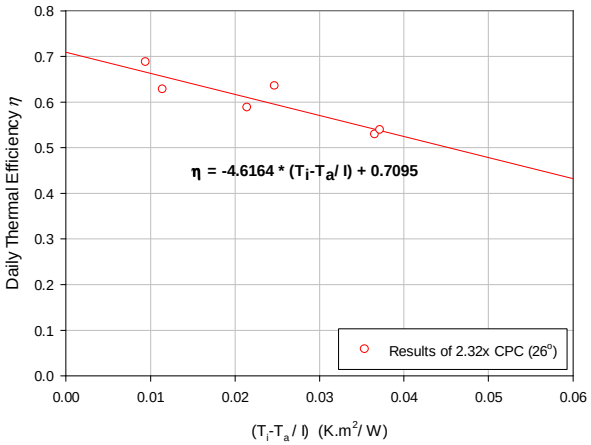

Fig. 17. Thermal efficiency curve of 2.32× CPC (26°).

4.3. Effect of truncation on the performance of 3.86× CPC (20°)

The truncation of CPC and its effect on the performance has been studied, for a number of reasons. First, the acceptance of beam and of diffuse insolation increases with truncation. Second, the average number of reflections decreases, and hence the optical efficiency increases, with truncation. Third, heat losses per aperture area increase with truncation.

Fig. 18 shows the variation of thermal efficiency, thermal losses and optical efficiency with the concentration ratio of 3.86× CPC truncated in three levels. As the concentration ratio decreases from (3.93× to 1×). Three empirical equations for thermal efficiency, thermal losses and optical efficiency of 3.86× CPC have been found from experimental tests to predict the performance curve of CPC at any concentration ratio between (1×-3.93×).

$$\eta_{th} = -0.0533 * C + 0.6837 \quad \ldots(14)$$

$$U_L = -1.9186 * C + 9.1274 \quad \ldots(15)$$

$$\eta_o = -0.1036 * C + 0.9012 \quad \ldots(16)$$

The empirical equations above, are used for full CPC with acceptance half angle (15°).

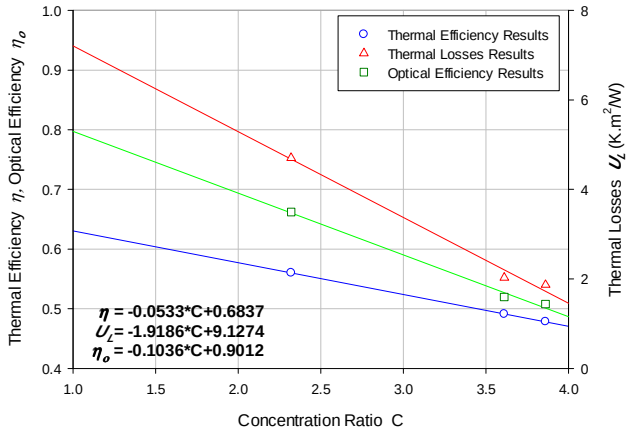

Fig. 18. Variation of optical and thermal performance and thermal losses with the concentration ratio of 3.86× CPC (20°).

5. Conclusions

From this work, the following conclusions are drawn:

1. The comparative studies have shown that the optimum acceptance half-angle is (θ_c=26°) for full CPC, not for truncated one.
2. Experimental results have shown that the maximum thermal efficiency of the full CPC with (C=2.32×) and (θc=26o) is 0.708.
3. The maximum thermal efficiency of the full CPC with (C=3.93×) and (θc=15o), when it's truncated to (C=3.84× and θc=20o), (C=3.61× and θc=26o) and (C=2.32× and θc=59o) are 0.51, 0.52 and 0.66, respectively.
4. The best concentration ratio of 3.93× CPC (θc=15o) is (C=2.32×) and (θc=59o).
5. Comparative studies show that the 2.32× CPC (θc=59o) has a good agreement with the performance of 2.32× CPC (θc=26o).
6. Empirical equations for optical and thermal efficiencies and thermal losses of 3.93× CPC (θc=15o) have been found over the concentration ratio.

Notation

A_a aperture area, m^2
C concentration ratio, dimensionless
c_p specific heat, J/kg. K
I_t hourly total irradiation, J/m^2
$\dot{m}$ mass flow rate, kg/s
Q_u useful heat gain, W
T_a ambient temperature, ^oC
T_i receiver inlet temperature, ^oC
T_o receiver outlet temperature, ^oC
U_L heat loss coefficient, m^2.K/W

Greek letters

η_{th} thermal efficiency, dimensionless
η_o optical efficiency, dimensionless
θ incidence ingle, degree
θ_c acceptance half-angle of CPC, degree
θ_l longitudinal projection angle
θ_l transversal projection angle

6. References

[1] Rabl A, "Solar Concentrators with Maximal Concentration for Cylindrical Absorbers". Applied Optics, vol. 15, pp. 1871-1873, 1976.

[2] Kalogirou S. A, "Solar Energy Engineering Processes and Systems", (2nd edition), Academic Press, San Diego, 2014.

[3] McIntire W. R, "Truncation of non-imaging cusp concentrators". Solar Energy, vol. 23, pp. 351-355, 1979.

[4] Gordon J. M., Carvalho-Pereira M., Rabl A., and Winston R, " Truncation of CPC solar collectors and its effect on energy collection". Solar Energy, vol. 35, pp. 393-399, 1985.

[5] Suzuki A., and Kobayashi, S, "Yearly Distributed Insolation Model and Optimum Design of a Two Dimensional Compound Parabolic Concentrator". Solar Energy, vol. 54, pp. 327-331, 1995.

[6] Winston R., and O'Gallagher J, " Non-Imaging Concentrators", In: Meyers, R. ed, Encyclopedia of Physical Science and Technology, Ch. Optics, pp. 507-522, Academic press, San Diego, 2004.

[7] Tang R., Wu M., Yu Y, and Li, M, "Optical Performance of Fixed East-West Aligned CPCs Used in China". Renewable Energy, vol. 35, pp. 1837-1841, 2010.

[8] Budihardjo I., Morrison L, "Performance of water-in-glass evacuated tube solar water heaters". Solar Energy, vol. 83, pp. 49-56, 2009.

[9] Kim Y. S., Balkoski K., Jiang L., and Winston R, "Efficient Stationary Solar Thermal Collector Systems Operating at a Medium-Temperature Range". Applied Energy, vol. 111, pp. 1071-1079, 2013.

[10] Trace Pro manual.

[11] Garg, H. P., and Prakash, J, "Solar Energy Fundamentals and Applications", (1st revised edition), Tata McGraw-Hill, New Delhi, 2008.

[12] ASHRAE Standard 93-2010, "Method of Testing to Determine the Thermal Performance of Solar Collectors", American Society of Heating Refrigerating and Air-conditioning Engineers, Atlanta, GA, 2014.

دراسة تجريبية لأداء مُركِّز شمسي على شكل قطع مُكافئ مُركَّب

قصي جهاد عبدالغفور* محمد عزيز حسن**

*،** قسم الهندسة الميكانيكية / الجامعة التكنولوجية

* البريد الالكتروني: kaisyqj@yahoo.com

** البريد الالكتروني: mohammedeng37@gmail.com

الخلاصة

تم عرض تصميم، تركيب والتحقيق في دراسة تجريبية لاثنين من المُركِّزات الشمسية المُركَّبة على شكل قطع مُكافئ ذي مستلم أنبوبي. تم تقويم أداء المركزين الشمسيين باستخدام القياسات التجريبية في الهواء الطلق بما في ذلك الكفاءة الحرارية اللحظية. تم اختبار المركزين بعد تثبيتهما على هيكل مشترك. اجريت العديد من الاختبارات في هذا العمل باقتطاع عاكس واحد من المركزين في ثلاثة مستويات مختلفة. لكل اقتطاع تم تغيير نصف زاوية القبول (θ_c). ونصف زاوية القبول المعيارية للمُركِّزات الشمسي على شكل قطع مُكافئ مركب هو (26^o). لمستويات الاقتطاع للمركز الثاني 1 و 2 و 3 نصف زاوية القبول كانت 20^o، 26^o و59^o على التوالي. الفرق بين الكفاءة الحرارية اللحظية ل 3.86× CPC ($\theta_c = 20^o$) و 2.32× CPC ($\theta_c = 26^o$)، وبين CPC 3.61× ($\theta_c = 26^o$) وCPC 2.32× ($\theta_c = 26^o$) هو فرق كبير وواضح. لوحظ أن الفرق بين الكفاءة الحرارية اللحظية ل 2.32× CPC ($\theta_c = 59^o$) وCPC2.32× ($\theta_c = 26^o$) هو اختلاف صغير مقارنة مع الفرق في الحالات الأولى والثانية، والكفاءة الحرارية اللحظية ل CPC2.32× (26^o) كان أعلى من تلك التي للمركزات الشمسية الثلاثة الأخرى. أظهرت النتائج التجريبية أن أقصى كفاءة حرارية ل CPC2.32× (26^o) الكامل مقدارها 0.708، أقصى كفاءة حرارية ل 3.93× CPC (15^o) ، عندما يكون مقتطعا إلى 3.84× CPC (20^o)، 3.61× CPC (26^o) و 2.32× CPC (59^o) مقدارها 0.51، 0.52 و 0.66 على التوالي. بنقصان نسبة التركيز من (3.93× الى1×)، الكفاءة الحرارية، الخسائر الحرارية والكفاءة البصرية ازدادت من (0.47 الى 0.63)، (1.58 الى 7.2 $K.m^2/W$) و(0.494 الى 0.797).